



Originally published as:

Groß, K., Micksch, U., and TIPTEQ Research Group, S. T., Araneda, M., Bataille, K., Bribach, J., Buske, S., Krawczyk, C. M., Lüth, S., Mechie, J., Schulze, A., Shapiro, S. A., Stiller, M., Wigger, P., Ziegenhagen, T. (2008): The reflection seismic survey of project TIPTEQ - the inventory of the Chilean subduction zone at 38.2° S. - *Geophysical Journal International*, 172, 2, pp. 565—571.

DOI: <http://doi.org/10.1111/j.1365-246X.2007.03680.x>

## FAST TRACK PAPER

# The reflection seismic survey of project TIPTEQ—the inventory of the Chilean subduction zone at 38.2° S

K. Groß,<sup>1</sup> U. Micksch<sup>2</sup> and TIPTEQ Research Group, Seismics Team\*

<sup>1</sup>Freie Universität Berlin, Fachrichtung Geophysik, Malteserstr. 74-100, 12249 Berlin, Germany. E-mail: kolja@geophysik.fu-berlin.de

<sup>2</sup>GeoForschungsZentrum Potsdam, Section Lithosphere Dynamics, Telegrafenberg, 14473 Potsdam, Germany

Accepted 2007 November 5. Received 2007 October 19; in original form 2007 May 25

## SUMMARY

We describe results of an active-source seismology experiment across the Chilean subduction zone at 38.2°S. The seismic sections clearly show the subducted Nazca plate with varying reflectivity. Below the coast the plate interface occurs at 25 km depth as the sharp lower boundary of a 2–5 km thick, highly reflective region, which we interpret as the subduction channel, that is, a zone of subducted material with a velocity gradient with respect to the upper and lower plate. Further downdip along the seismogenic coupling zone the reflectivity decreases in the area of the presumed 1960 Valdivia hypocentre. The plate interface itself can be traced further down to depths of 50–60 km below the Central Valley. We observe strong reflectivity at the plate interface as well as in the continental mantle wedge. The sections also show a segmented forearc crust in the overriding South American plate. Major features in the accretionary wedge, such as the Lanalhue fault zone, can be identified. At the eastern end of the profile a bright west-dipping reflector lies perpendicular to the plate interface and may be linked to the volcanic arc.

**Key words:** Controlled source seismology; Subduction zone processes; Continental margins: convergent; Dynamics: seismotectonics; South America.

## 1 INTRODUCTION

One of the main goals in subduction zone research is to understand the structural and petrophysical properties of seismogenic coupling zones, especially their downdip end. Here, mega-thrust earthquakes are inferred to initiate, but the triggering mechanisms and processes are still poorly understood (e.g. Bebout *et al.* 1996; Oleskevich *et al.* 1999; Peacock & Hyndman 1999; Stern 2002; Nicholson *et al.* 2005). All subduction earthquakes with magnitudes larger than eight occur in the seismogenic coupling zone, often located close to the coast where population is concentrated. Therefore, coastal areas above subduction zones are subject to high-risk potential.

With a quarter of the worldwide seismic energy in the last century having been released in the Chilean region alone (Scholz 2002), the Andean subduction zone is a natural laboratory for our seismogenic-zone studies. The overarching purpose of project TIPTEQ (from The Incoming Plate to mega-Thrust Earthquake processes), which com-

prises 13 subprojects, is to investigate processes active at all scales in the seismogenic coupling zone in south central Chile (Fig. 1), which hosted the rupture plane of the 1960 Valdivia earthquake ( $M_w = 9.5$ ; Cifuentes 1989; Barrientos & Ward 1990). The controlled-source seismology survey described here aims at imaging and identifying the structural properties within the seismogenic coupling zone at 38.2°S.

In this manuscript, we summarise the experiment setup and field acquisition. Then we present structural images including an initial interpretation of the observed features below this part of the Chilean forearc.

## 2 SURVEY SETUP

The TIPTEQ survey was conducted at 38.2°S and trended W–E, crossing the Coastal Cordillera, where the 1960 earthquake hypocentre is thought to have occurred (Cifuentes 1989; Krawczyk & the SPOC Team 2003), and the western portion of the Central Valley (Fig. 1). The experiment was cored by a 95.5 km long near-vertical reflection (NVR) survey with explosive shots every 1.5 km and three-component geophones every 100 m (see Table 1). Three shots off the end of the line extended it eastwards to a total length of 118 km. The NVR survey was supplemented by an expanding spread profiling (ESP) component, consisting of 15 extra shots with

\*Groß, K., FU Berlin, Germany (a); Micksch, U., GFZ Potsdam, Germany (b); Arandeda, M., SEGMI, Santiago, Chile (c); Bataille, K., Universidad de Concepción, Chile (d); Bribach, J. (b); Buske, S. (a); Krawczyk, C.M. (b); Lüth, S. (a,b); Mechie, J. (b); Schulze, A. (b); Shapiro, S.A. (a); Stiller, M. (b); Wigger, P. (a); Ziegenhagen, T. (b).

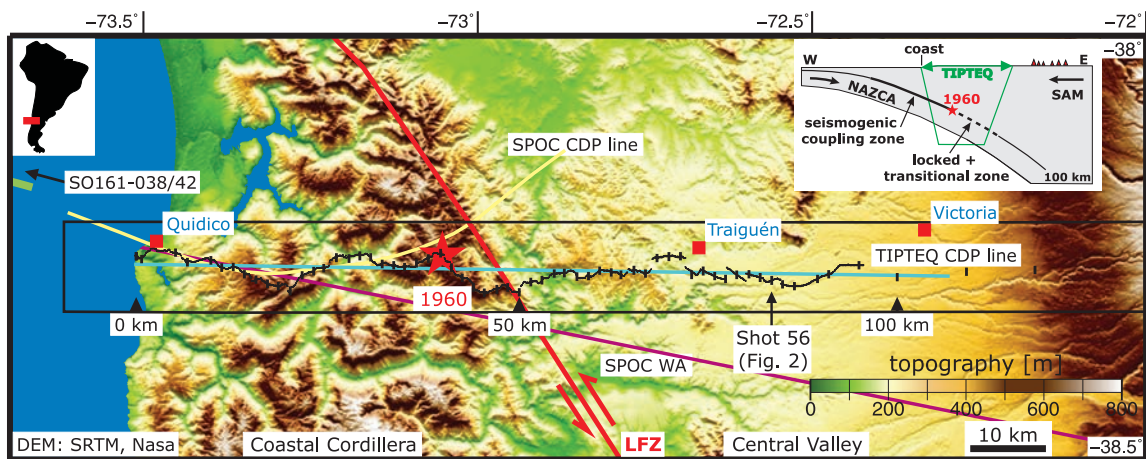


**Figure 1.** Location map of the active-source seismological experiment of project TIPTEQ (for acquisition details see Table 1). Black line – receiver line, black ticks – shot locations, blue line – CDP line, black box – Kirchhoff migration volume (cf. Fig. 4 and text), red star – hypocentral area of the 1960 earthquake. The yellow and magenta lines mark the CDP line of the SPOC onshore seismic reflection profile and the SPOC wide-angle refraction profile, respectively (Krawczyk & the SPOC Team 2003). The green line marks the eastern end of the marine seismic reflection profile SO161-038/42 (Reichert & Schreckenberger 2002). The red line maps the surface trace of the Lanahue fault zone (LFZ; after Melnick & Ehtler 2006). NAZCA and SAM in the inset label the Nazca and South American plates, respectively.

offsets up to almost 100 km, and focussing on the downdip end of the seismogenic coupling zone 20–50 km inland at about 45 km depth. In a pilot study the generation of horizontally polarized shear waves (*SH* waves) using the three-hole (Camouflet) method (Dohr (1985)) was tested.

Within project Subduction Processes Off Chile (SPOC; Krawczyk & the SPOC Team 2003; Krawczyk *et al.* 2006; Sick *et al.* 2006) an onshore seismic reflection profile with a two-fold common depth-point (CDP) coverage served as a feasibility study for the survey described here. The two profiles coincide along the first 45 km eastwards of the coast. Then the SPOC profile turns northwards for another 10 km, while the TIPTEQ profile continues east for about 50 km. Furthermore, the onshore profiles connect westwards to an existing marine seismic reflection profile, which yields a high resolution image of the subducted oceanic plate and the trench region (Reichert & Schreckenberger 2002; Rauch 2005) (see Fig. 1).

### 3 DATA PROCESSING AND RESULTS

Single shot gathers (e.g. Fig. 2) show distinct reflections (e.g. between 4 and 5 s two-way time (TWT)) and broad reflectivity bands (e.g. below 6 s TWT down to at least 17 s TWT). These bands have different dips and continue laterally over several kilometres. For the shot record shown in Fig. 2 the reflectivity around 15–17 s TWT is associated with the plate interface and will be characterized in the further interpretation.

The SPOC wide-angle refraction experiment provided us with a *P*-wave velocity model (Krawczyk & the SPOC Team 2003, Fig. 3) along the same latitude (Fig. 1). This velocity information was used to produce a CDP stacked time section and a pre-stack depth migrated section of the vertical component of the NVR data set (Fig. 4). The processing and the major structural features of both sections are described below.

#### 3.1 The CDP stacked time section

To produce a brute stack of the NVR data the processing comprised the following steps. After data-conversion and assigning the field

geometry, the NVR data were edited for bad traces, traces with reversed polarity and GPS timing errors. The data were bandpass-filtered and spherical divergence losses were recovered by two offset-dependent amplitude correction operators. Horizontal scaling (trace equalization) and automatic gain control (AGC) were applied, as well as a lateral coherency enhancement. After normal move-out (NMO) correction, a CDP reflectivity stack with phase restoration was carried out, including horizontal and vertical trace balancing.

The resulting time section (Fig. 4a) shows coherent reflections and broad reflectivity bands throughout the section. A prominent continuous reflector band is visible between 9 s TWT at the coast and 17 s TWT under the Central Valley. From 0 to 10 s TWT, the seismic section is strongly structured between the coast and the Central Valley showing dipping, horizontal and arched bands of high reflectivity with a duration of 1–2 s TWT. These distinct reflective bands are structurally continuous for tens of kilometres distance. An enigmatic reflection is present below 20 s TWT in the eastern half of the section.

#### 3.2 The pre-stack depth migrated section

Kirchhoff pre-stack depth migration was performed in a 3-D volume (see box in Fig. 1) using the true source and receiver coordinates, thereby taking into account the actual crooked line geometry and the topography along the profile using the method of Buske (1999). As input velocities for the migration we used a smoothed version of the SPOC 2-D wide-angle velocity model (see Fig. 3) that was stretched in N–S direction in order to provide a 3-D model. The single shot gathers were migrated separately using the true phase information. Then trace envelopes of all migrated single shots were calculated and stacked to form a 3-D image. An analysis of the 3-D migration volume showed almost no structural dip perpendicular to the survey line. That allowed us to further increase the signal-to-noise ratio up to a factor of 2 by summing of the W–E oriented depth slices. The resulting 2-D depth section is shown in Fig. 4(b). For further details concerning the process of crossline stacking see Yoon *et al.* (2003) and Yoon (2005). More details on the concept of crooked line migration in 2-D and 3-D in general can be found in Nedimović & West (2003a,b).

**Table 1.** Acquisition and field parameters of the controlled-source seismology experiment of the TIPTEQ project.

General information	
Recording period	2005 January 13–30
Area	Southern central Chile, ~38.2° S, 73.5–72° W
Profile length	105-km-long CDP line
Total data amount	Three components, 1.5 GB each
Recording	
Recording system	Portable field recorders, EarthDataLogger PR6-24 (GPS-clock, 6–40 GB HDs)
Sampling rate	5 ms
Recording format	MiniSEED, continuous
Extracted event time	102 s
Receivers	
Number of channels	180
Geophone type	Three-component geophone, Sensor P-6/B, 4.5 Hz
Geophones/station	1 (buried)
Geophone spacing	100 m (projected on CDP line)
Spread length	18.0 km
Daily roll-along	4.5 km (east to west)
Number of stations	955
Sources	
Source type	Explosive shots in boreholes
Explosive charge/shot	
NVR, SH	75 kg (1 hole, 20 m deep)
East off the line	100/150/200 kg (1/2/2 Holes; 25/20/25 m deep)
ESP	150–300 kg (2 holes, 20–30m deep)
Shot spacing	
NVR/SH/ESP	1.5/9.0/9.0 km
Number of shots	
NVR/SH/ESP	73/13/15
East off the line	3 (all during first set-up)
Subsurface coverage	
NVR/SH/ESP	8/1/10-fold (nominal)

An east-dipping reflective band with a thickness of 2–5 km appears below the coast at a depth of about 25 km. Apart from a region of low reflectivity at  $x = 30$ –50 km, this reflective band can be traced down to a depth of 50 km below the Central Valley. The upper boundary of this reflective band is relatively diffuse whereas the lower boundary appears comparatively sharp. The section above this reflective band from  $x = 0$ –30 km shows several discrete, bent and horizontal reflectors. The region from  $x = 30$ –50 km shows little and diffuse reflectivity. From  $x = 50$ –90 km a highly reflective region can be observed which continues up to 15–20 km depth where it is bounded by an almost transparent area. Within this region predominantly horizontal structures are visible. At the eastern end of the profile from 40 to 70 km depth a strong west-dipping reflector appears almost perpendicular to the downward prolongation of the east-dipping reflective band. An extension to shallower depths cannot be imaged due to the eastern limit of the profile.

#### 4 INTERPRETATION AND DISCUSSION

Fig. 4(c) shows a preliminary interpretation based on the post-stack and pre-stack images. The sharp lower boundary of the reflective band between 25 km depth at the coast and 50 km depth below the Central Valley (Fig. 4b) is interpreted as the top of the subducted ma-

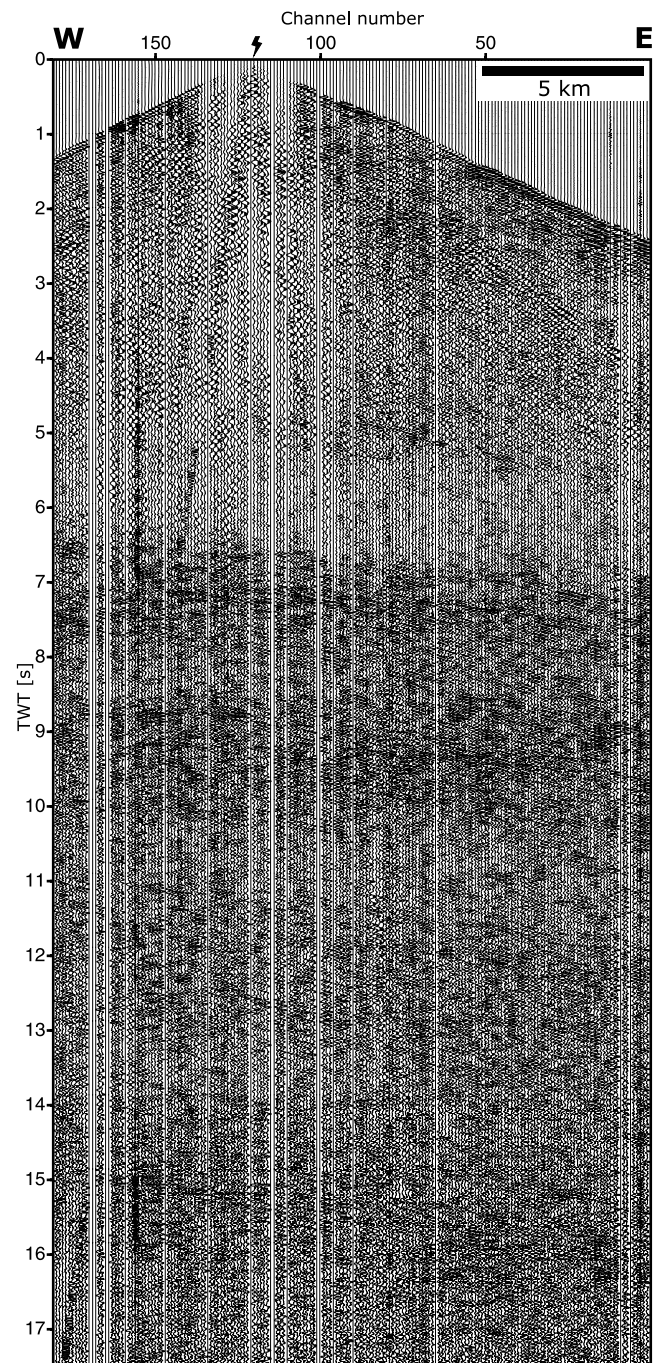


**Figure 2.** NVR shot gather (shot no. 56; marked by spark) recorded along the asymmetric 18-km-long geophone spread (for location see Fig. 1). The section shows the vertical component of ground motion. It has only been bandpass-filtered and horizontally and vertically scaled, underlining the good data quality.

terial going down with the velocity of the Nazca plate. This boundary coincides with the plate interface in the SPOC wide-angle velocity model, which was inferred from the observed oceanic Moho and the thickness of the oceanic crust imaged by marine seismics close to the coast.

The reflectivity from  $x = 0$  to 30 km directly above the plate boundary can be associated with the existence of a subduction channel (Lohrmann *et al.* 2006; Krawczyk *et al.* 2006) with a thickness of 2–5 km (Fig. 4c). The subduction channel as defined by Cloos

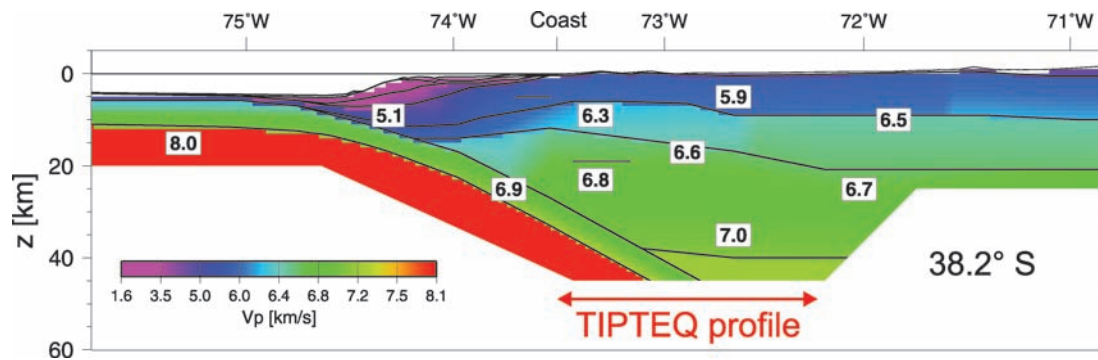


**Figure 3.** Wide-angle  $P$ -wave velocity model of profile SPOC-South showing the geometry of the downgoing plate and the velocity structure at  $38.2^\circ$  S (modified after Krawczyk & the SPOC Team 2003).

& Shreve (1988) is a zone with varying thickness above the oceanic crust in which material being transported downwards, exhibits a velocity gradient with respect to both plates. The material flowing within the subduction channel is derived from trench deposits, off scrapings from the base of the upper plate by tectonic erosion, or from the top of the downgoing plate at depth. Following this concept we expect the subduction channel and the transition zone to be highly reflective, as material here differs from its surroundings, thus inducing a strong impedance contrast. An additional process leading to high reflectivity may be the dewatering of sediments carried down in the subduction channel and the migration of fluids into the continental crust. Currently the thickness of the subducting sediments is 2.2 km at the trench (Rauch 2005), but this is neither expected to be continuous along the entire subduction channel nor through time. The thickness of 2–5 km of the subduction channel we observe onshore is an upper bound, as we cannot distinguish material within the subduction channel from freshly accreted material or material that is moving with the oceanic plate. According to Cloos & Shreve (1988) a narrowing of the subduction channel leads to an upflow of material, and thus causes a thickening of the channel further up-dip. This process is one possible explanation for basal accretion. We observe such a thickening of the channel ( $>2$  km;  $x = 15$ – $20$  km) below the Coastal Cordillera, where uplift is observed and attributed to basal accretion by Glodny *et al.* (2005). The authors conducted a detailed study in the Valdivia area using isotope tectonochronology and sandbox modelling. This study shows that the intercalated metasediments and metabasites which build up the Coastal Cordillera at the surface were once basally accreted and consist of material that was transported from the offshore trench to depth along what is thought to be the subduction channel. In our sections we observe a strongly segmented upper plate showing horizontal and arched reflector elements that characterize the internal structure of the Permo-Triassic accretionary wedge, tracing at depth the sequences mapped and dated at the surface. The melange in the channel that is subducted further down undergoes dehydration and embrittlement and may lead to the observed reflectivity at  $x = 50$ – $90$  km at depths of 42–55 km. Local seismicity studies (Haberland *et al.* (2006)) show moderate seismic activity along the plate interface as well as within the supposed subduction channel.

The varying pattern of reflectivity observed in the overriding plate can be explained in the context of local geology (e.g. Hérve 1988) and morphotectonic segmentation of the region (e.g. Mpodozis & Ramos 1989; Melnick & Echtler 2006). At  $x = 51$  km the profile crosses the Lanalhue fault zone (LFZ). Its continuation to about 10 km depth can be inferred by a lateral change of reflectivity (Figs 4a and b). A granite body covered by sediments of the Eastern

Series (Hérve 1988) occurs east of the LFZ and causes an almost transparent image down to 20 km depth, where an east-dipping reflector indicates a change to highly reflective material. This high reflectivity may be caused by fluids trapped just below the granite or simply by a change in the lithology. The Western Series (Hérve 1988) is made up of chlorite schists, which are exposed towards the coast, and a more heterogeneous basement devoid of sediments in the Coastal Cordillera. Both the schists and the homogeneous granite body are favourable for deep seismic imaging, whereas due to scattering absorption it is probably difficult to image structures below the strongly heterogeneous basement. This situation is one possible explanation for the less reflective central part of the section (Figs 4a and b).

A clear boundary marking the position of the continental Moho could not be found in the NVR data. The dewatering of the downgoing oceanic crust might lead to serpentinized forearc mantle material that reduces the velocity contrast between continental crust and mantle and thus hampers the formation of an explicit Moho reflection in the seismic image. This phenomenon is also observed in receiver function data from the Cascadia subduction zone (Bostock *et al.* 2002; Nicholson *et al.* 2005) and Alaska (Abers *et al.* 2006). Constraints from a thermal model (e.g. isotherm geometries and phase transitions) are not available yet, but it is an ongoing effort within project TIPTEQ to construct such a model for this region for the first time.

Even though the existence of the continental Moho within the overriding plate is not directly evident, we can consider two possible delineations and intersections of the continental Moho with the oceanic plate from the seismic image. The first scenario assumes the hypocentre of the 1960 Chile earthquake as shown in the section in Fig. 4(c) after Krawczyk & the SPOC Team (2003). The authors relocated the hypocentre using the continental Moho from the SPOC wide-angle velocity model (Fig. 3) together with the assumption that the hypocentres of mega-thrust earthquakes initiate at the downdip end of seismogenic coupling zones (e.g. Oleskevich *et al.* 1999; Peacock & Hyndman 1999). Engdahl & Villaseñor (2002) relocated the 1960 earthquake epicentre independently at almost the same location (within 4 km horizontal distance) using an improved global velocity model (ak135) and a new location procedure (EHB method). The reflectivity east of the 1960 hypocentre shows horizontal structures at various depths that may be linked to a continental Moho (see Fig. 4c). We may see a horizontal Moho at 38 km depth as indicated in the SPOC wide-angle data or a Moho rising up to a depth of 32, respectively, 25 km. The highest position would coincide with the interpretation of Yuan *et al.* (2006) based on receiver function studies at  $\sim 39^\circ$ S.

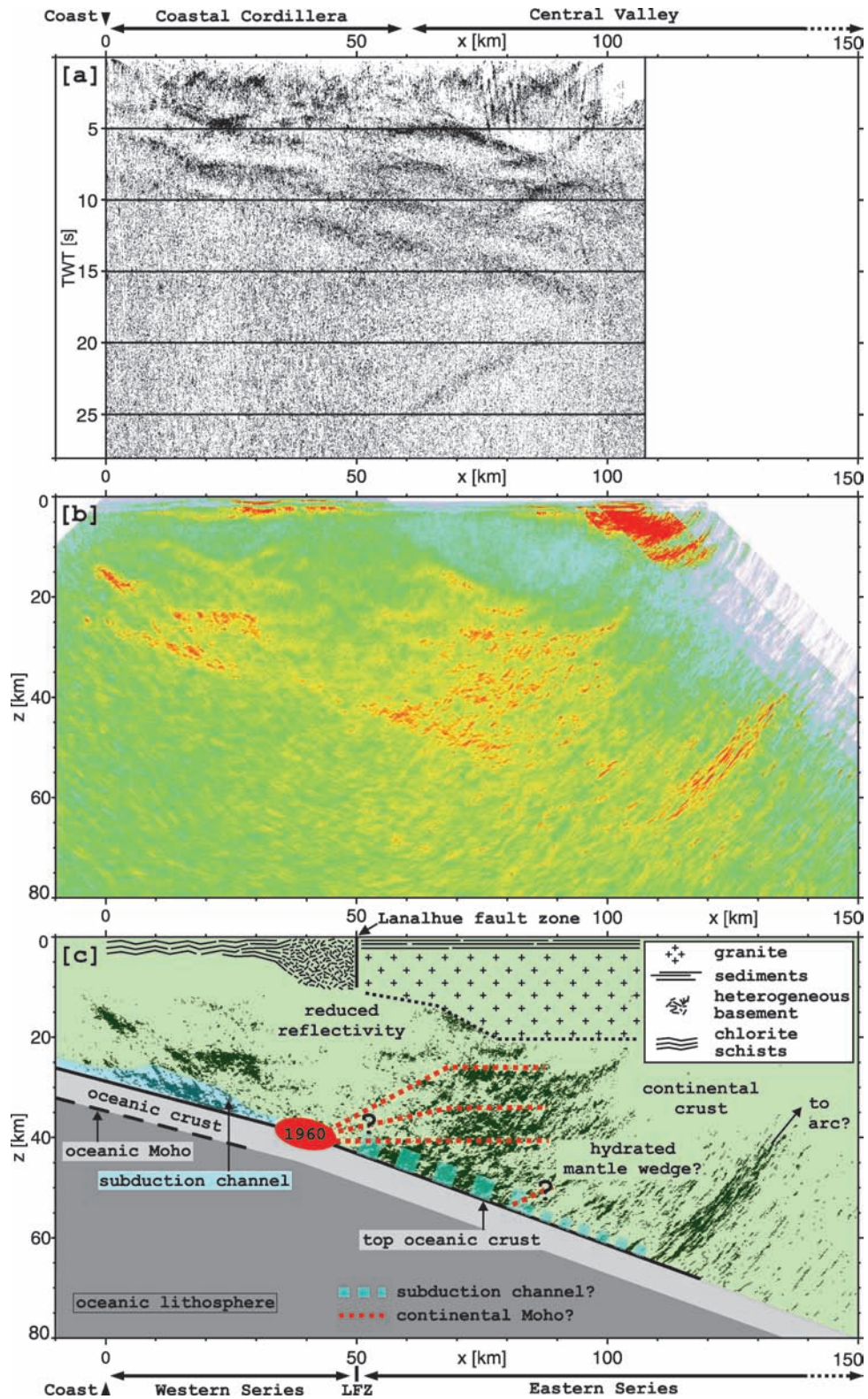


**Figure 4.** TIPTEQ profile at 38.2°S as (a) Unmigrated post-stack time section; (b) Kirchhoff pre-stack depth migrated section; (c) Preliminary interpretation with the region of the 1960 earthquake hypocentre marked. See text for details.

The second possibility is, that we do not directly image the continental Moho, because it encounters the oceanic plate at depths greater than 50 km. We cannot image horizontal or east dipping structures with high coverage in these depths east of profile-km 80

due to the experiment geometry. This would imply that all of the reflectivity above the plate interface is attributed to the continental crust and the location of the 1960 earthquake is not at the intersection of the continental Moho with the oceanic crust. However, a

continental Moho depth of 50 km or more would be highly surprising as the continental Moho, if anything, tends to shallow towards the coast from the present-day topographically high, volcanic arc of the Andes beneath which it does not reach depths of more than 40–50 km between 37° and 39°S (Krawczyk *et al.* 2006). If the continental Moho were to intersect the oceanic plate at depths greater than 50 km, then crustal material should have been added to the base of the crust in this region. As a consequence, one would expect this region to uplift due to isostasy. However, presently this region occupies the western part of the topographically low central valley. Thus it seems unlikely that the continental Moho intersects the oceanic plate at depths greater than 50 km.

Significant changes in reflectivity along the plate interface are also reported in other subduction systems. In Cascadia, Nedimović *et al.* (2003) suggest a correlation between reflectivity and coupling along the plate interface. According to their interpretation, a thin reflective zone less than 2 km thick indicates the coupled section of the plate interface. This zone broadens to 2–4 km in a transitional zone at the downdip end of the seismogenic coupling zone. A broad reflection band more than 4 km thick (E-layer) marks the beginning of the zone of aseismic creep. For south central Chile we observe a similar thickness variation in the reflective zone along the plate interface from an average thickness of 2–3 km in the coupled zone at 24–36 km depth to more than 4 km in the zone of aseismic creep at 40–55 km depth (Fig. 4). However, instead of a gradual thickening in the transitional zone from 36 to 40 km depth, we observe a zone of low reflectivity as discussed above. In Cascadia the reflections from the E-layer vanish where the oceanic plate encounters the mantle wedge. In our preferred interpretation of the TIPTEQ seismic data with the onset of the continental Moho at 38 km depth, the reflectivity corresponding to the E-layer starts at the beginning of the mantle wedge. We attribute this reflective band to the continuation of the subduction channel towards depth. A similar observation is reported by Calvert *et al.* (2003) for Cascadia where a lobe of subducted material and sheared crustal rocks, up to 15 km thick, underplates the serpentinized mantle wedge.

The origin of the E-layer in the Cascadia subduction zone was addressed by several authors. Green *et al.* (1986) interpret the laminated structure of the E-layer as the lowermost layers of lithified sediments and possibly the uppermost crystalline layers of the oceanic crust underplating the base of the overriding plate, whereas Nicholson *et al.* (2005) attribute the E-layer to fluids in the upper part of the oceanic crust. A migration of these fluids into the continental crust can explain variations in the thickness of the layer. This is in agreement with Kurtz *et al.* (1986) who modeled a zone of high electrical conductivity at the depth of the seismic E-horizon caused by saline fluids in the pore spaces of sedimentary and mafic materials of the upper oceanic crust. All three papers place the E-layer at the plate interface between the upper part of the oceanic crust and the base of the continental crust and connect it with processes active at the plate interface. These findings from Cascadia support our interpretation of the reflective band at the plate interface as the seismic signature of the fluid filled subduction channel in south central Chile. Other studies in Cascadia argue that the E-layer reflection is caused by fluids trapped at a boundary in the continental crust at least 10 km above the plate interface (e.g. Hyndman 1988). This is further supported by receiver function analysis (Cassidy & Ellis 1993) and a 3-D compressional wave velocity model constructed through tomographic inversion (Ramachandran *et al.* 2005). In this interpretation the top of the oceanic plate is correlated with a thin reflective band (F-layer) below the E-layer. With our available data for south central Chile the depth of the plate interface is well constrained. The

E-layer as interpreted above might correspond in our case to strong subhorizontal reflections in the continental crust (e.g. from  $x = 10$  to 50 km and  $z = 25$  to 30 km in Fig. 4b).

The nature and the origin of the bright west-dipping reflector at the eastern end of the profile at 40–70 km depth (Fig. 4) is not yet clear. We note the spatial coincidence of its extrapolation to the surface and the trace of the Liquiñe-Ofqui fault zone, which is a transpressional feature at the magmatic arc (Hérve 1994; Rosenau *et al.* 2006). One might speculate that this bright reflective feature is related to a possible ascent path for melts towards the volcanic arc. The position of the reflector also coincides with a local anomaly in the  $P$ -wave velocity model derived from local earthquake tomography (Bohm 2004; Asch *et al.* 2006).

## 5 SUMMARY

We present a structural image and a first interpretation of the NVR data set of project TIPTEQ, acquired across the seismogenic coupling zone of the south central Chilean subduction zone. The image clearly shows the subducted oceanic Nazca plate below the segmented forearc and a highly reflective overriding South American plate. We associate the high reflectivity at the plate interface with the existence of a subduction channel with a varying thickness of 2–5 km down to a depth of at least 38 km. It might continue towards depth. The continental Moho is not clearly imaged. However, one possible location is at 38 km depth given by the 1960 earthquake hypocentre. The reflectivity east of the hypocentre shows horizontal structures at various depths, which give rise to different eastward continuations of the continental Moho. The position and extent of the continental mantle wedge changes accordingly. Major forearc features such as the crustal Lanalhue fault zone and a strong west-dipping reflector perpendicular to the plate interface, can be observed.

Future research will be directed towards further advanced processing and imaging as well as the incorporation of the ESP and  $SH$ -waves components of the survey. Furthermore, the existing velocity model from project SPOC will be improved by using the ESP data and first-break tomography. Finally, the results provide a framework for further analysis of the corresponding subduction related processes in south central Chile and will enter an integrative interpretation within the whole TIPTEQ project.

## ACKNOWLEDGMENTS

We thank Nathan L. Bangs, Anne M. Tréhu, Mladen Nedimović, colleagues and an anonymous reviewer for intense discussion and constructive reviews, thereby improving the manuscript. This is publication no. GEOTECH-211 of the R&D-Program GEOTECHNOLOGIEN funded by the German Ministry of Education and Research (BMBF) (Grant 03G0594) and the German Research Foundation (DFG). The project benefited from grants of the Freie Universität Berlin and the GFZ Potsdam; seismic stations were provided by the Geophysical Instrument Pool Potsdam and the Freie Universität Berlin. We thank drilling contractor Detroman (Concepción) as well as all participants in the field and the Chilean inhabitants for having made this survey possible.

## REFERENCES

- Abers, G., van Keken, P., Kneller, E., Ferris, A. & Stachnik, J., 2006. The thermal structure of subduction zones constrained by seismic imaging: implications for slab dehydration and wedge flow, *Earth planet. Sci. Lett.*, **241**, 387–397.

- Asch, G. *et al.*, 2006. Seismological studies of the Central and Southern Andes, in *The Andes—Active Subduction Orogeny. Frontiers in Earth Sciences*, Vol. 1, pp. 443–457, eds Oncken, O., Chong, G., Franz, G., Giese, P., Götze, H., Ramos, V., Strecker, M. & Wigger, P., Springer Verlag, Berlin.
- Barrientos, S. & Ward, S., 1990. The 1960 Chile earthquake: inversion for slip distribution from surface deformation, *Geophys. J. Int.*, **103**, 589–598.
- Bebout, G., Scholl, D., Kirby, S. & Platt, J., 1996. *Subduction: Top to Bottom*, *Geophys. Monogr. Ser.*, 96. AGU, Washington DC., 384 pp.
- Bohm, M., 2004. 3-D Lokalbeben-tomographie der südlichen Anden zwischen 36° und 40°S, *PhD thesis*, Freie Universität Berlin, Scientific Technical Report STR04/15, GFZ Potsdam, Potsdam, 136 pp., <http://www.diss.fu-berlin.de/2005/7/>, <http://www.gfz-potsdam.de/bib/pub/str0415/0415.pdf>.
- Bostock, M., Hyndman, R., Rondenay, S. & Peacock, S., 2002. An inverted continental Moho and serpentinization of the forearc mantle, *Nature*, **417**, 536–538.
- Buske, S., 1999. Three-dimensional pre-stack Kirchhoff migration of deep seismic reflection data, *Geophys. J. Int.*, **137**, 243–260.
- Calvert, A., Fisher, M., Ramachandran, K. & Tréhu, A., 2003. Possible emplacement of crustal rocks into the forearc mantle of the Cascadia Subduction Zone, *Geophys. Res. Lett.*, **30**(23), 2196.
- Cassidy, J. & Ellis, R., 1993. S wave velocity structure of the Northern Cascadia subduction zone, *J. geophys. Res.*, **98**(B3), 4407–4421.
- Cifuentes, I., 1989. The 1960 Chilean earthquake, *J. geophys. Res.*, **94**(B1), 665–680.
- Cloos, M. & Shreve, R., 1988. Subduction-channel model of prism accretion, melange formation, sediment subduction, and subduction erosion at convergent plate margins: 1. Background and description, *Pageoph*, **128**, 455–500.
- Dohr, G., 1985. Development of a procedure for the exploration of areas with poor reflections by the combined application of different geophysical methods, taking the North-West German basin as an example, in *New Technologies for the Exploration and Exploitation of Oil and Gas Resources*, pp. 62–69, eds De Bouw R., Millich, E., Joulia, J. & Van Asselt, D., Graham and Trotman, London, United Kingdom.
- Engdahl, E. & Villaseñor, A., 2002. 41. Global Seismicity: 1900–1999, in *International Handbook of Earthquake & Engineering Seismology, Part A*, Vol. 81A, pp. 665–690, eds Lee, W., Kanamori, H., Jennings, P. & Kisslinger, C., Academic Press, Amsterdam.
- Glodny, J., Lohrmann, J., Gräfe, K., Seifert, W., Collao, S. & Figueroa, O., 2005. Internal dynamics of a paleoaccretionary wedge: insights from combined isotope tectonochronology and sandbox modelling of the South-Central Chilean forearc, *Earth planet. Sci. Lett.*, **231**, 23–39.
- Green, A., Clowes, R., Yorath, C., Spencer, C., Kanasewich, E., Brandon, M. & Sutherland Brown, A., 1986. Seismic reflection imaging of the subducting Juan de Fuca plate, *Nature*, **319**, 210–213.
- Haberland, C., Rietbrock, A., Lange, D., Bataille, K. & Hofmann, S., 2006. Interaction between forearc and oceanic plate at the South-Central Chilean margin as seen in local seismic data, *Geophys. Res. Lett.*, **33**(23), L23302.
- Hérve, F., 1988. Late Paleozoic subduction and accretion in Southern Chile, *Episodes*, **11**, 183–188.
- Hérve, F., 1994. The Southern Andes between 39 degrees and 44 degrees S latitude - the geological signature of a transpressive tectonic regime related to a magmatic arc, in *Andean Geodynamics. Frontiers in Earth Sciences*, pp. 243–248, eds Reutter, K., Scheuber, E. & Wigger, P., Springer Verlag, Berlin.
- Hyndman, R., 1988. Dipping Seismic Reflectors, Electrically Conductive Zones, and Trapped Water in the Crust Over a Subducting Plate, *J. geophys. Res.*, **93**(B11), 13 391–13 405.
- Krawczyk, C. & the SPOC Team, 2003. Amphibious seismic survey images plate interface at 1960 Chile earthquake, *EOS Trans. Am. geophys. Union*, **84**(32), 301, 304–305.
- Krawczyk, C. *et al.*, 2006. Geophysical Signatures and Active Tectonics at the South-Central Chilean Margin, in *The Andes—Active Subduction Orogeny. Frontiers in Earth Sciences*, Vol. 1, pp. 171–192, eds Oncken, O., Chong, G., Franz, G., Giese, P., Götze, H., Ramos, V., Strecker, M. & Wigger, P., Springer Verlag, Berlin.
- Kurtz, R., DeLaurier, J. & Gupta, J., 1986. A magnetotelluric sounding across Vancouver Island detects the subducting Juan de Fuca plate, *Nature*, **321**, 596–599.
- Lohrmann, J., Kukowski, N., Krawczyk, C., Oncken, O., Sick, C., Sobiesiak, M. & Rietbrock, A., 2006. Subduction channel evolution in brittle forearc wedges—a combined study with scaled sandbox experiments, seismological and reflection seismic data and geological field evidences, in *The Andes—Active Subduction Orogeny. Frontiers in Earth Sciences*, Vol. 1, pp. 237–262, eds Oncken, O., Chong, G., Franz, G., Giese, P., Götze, H., Ramos, V., Strecker, M. & Wigger, P., Springer Verlag, Berlin.
- Melnick, D. & Echtler, H., 2006. Morphotectonic and geologic digital map compilations of the south-central Andes (36–43°S), in *The Andes—Active Subduction Orogeny. Frontiers in Earth Sciences*, Vol. 1, pp. 565–568, eds Oncken, O., Chong, G., Franz, G., Giese, P., Götze, H., Ramos, V., Strecker, M. & Wigger, P., Springer Verlag, Berlin.
- Mpodozis, C. & Ramos, V., 1989. The Andes of Chile and Argentina, in *Geology of the Andes and its Relation to Hydrocarbon and Mineral Resources*, pp. 59–90, eds Ericksen, G., Pinochet, M. & Reinemund, J., Circumpacific Council for Energy and Mineral Resources, Earth Sciences Series, 11, Houston, TX.
- Nedimović, M. & West, G., 2003a. Crooked-line 2D seismic reflection imaging in crystalline terrains. Part 1: data processing, *Geophysics*, **68**(1), 274–285.
- Nedimović, M. & West, G., 2003b. Crooked-line 2D seismic reflection imaging in crystalline terrains. Part 2: migration, *Geophysics*, **68**(1), 286–296.
- Nedimović, M., Hyndman, R., Ramachandran, K. & Spence, G., 2003. Reflection signature of seismic and aseismic slip on the northern Cascadia subduction interface, *Nature*, **424**, 416–420.
- Nicholson, T., Cassidy, J. & Bostock, M., 2005. New constraints on subduction zone structure in northern Cascadia, *Geophys. J. Int.*, **161**, 846–859.
- Oleskevich, D., Hyndman, R. & Wang, K., 1999. The updip and downdip limits to great subduction earthquakes: thermal and structural models of Cascadia, south Alaska, SW Japan, and Chile, *J. geophys. Res.*, **104**(B7), 14 965–14 991.
- Peacock, S. & Hyndman, R., 1999. Hydrous minerals in the mantle wedge and the maximum depth of subduction thrust earthquakes, *Geophys. Res. Lett.*, **26**(16), 2517–2520.
- Ramachandran, K., Dosso, S., Spence, G., Hyndman, R. & Brocher, T., 2005. Forearc structure beneath southwestern British Columbia: a three-dimensional tomographic velocity model, *J. geophys. Res.*, **110**(B02303).
- Rauch, K., 2005. Cyclicity of Peru-Chile trench sediments between 36° and 38°S: a footprint of paleoclimatic variations?, *Geophys. Res. Lett.*, **32** (L08302).
- Reichert, C. & Schreckenberger, B., 2002. Cruise report SO-161 leg 2 & 3, SPOC (Subduction Processes Off Chile), Tech. rep., BGR Hannover, pp. 142.
- Rosenau, M., Melnick, D. & Echtler, H., 2006. Kinematic constraints on intra-arc shear and strain partitioning in the Southern Andes between 38° S and 42° S latitude, *Tectonics*, **25**, TC4013.
- Scholz, C., 2002. *The Mechanics of Earthquakes and Faulting*, Cambridge University Press, Cambridge, UK, 471 pp.
- Sick, C. *et al.*, 2006. Seismic images of accretive and erosive subduction processes from the Chilean margin, in *The Andes—Active Subduction Orogeny. Frontiers in Earth Sciences*, Vol. 1, pp. 147–169, eds Oncken, O., Chong, G., Franz, G., Giese, P., Götze, H., Ramos, V., Strecker, M. & Wigger, P., Springer Verlag, Berlin.
- Stern, R., 2002. Subduction zones, *Rev. Geophys.*, **40**(4), 1–38.
- Yoon, M.-K., 2005. Deep seismic imaging in the presence of a heterogeneous overburden. Numerical modelling and case studies from the Central Andes and Southern Andes, *PhD thesis*, Freie Universität Berlin, <http://www.diss.fu-berlin.de/2005/74/indexe.html>.
- Yoon, M., Buske, S., Lüth, S., Schulze, A., Shapiro, S., Stiller, M. & Wigger, P., 2003. Along-strike variations of crustal reflectivity related to the Andean subduction process, *Geophys. Res. Lett.*, **30**(4), 1160.
- Yuan, X. *et al.*, 2006. Deep Seismic Images of the Southern Andes, in *Evolution of an Andean Margin: A Tectonic and Magmatic View from the Andes to the Neuquen Basin (36–39°S)*, Vol. 407, pp. 61–72, eds Kay, S. & Ramos, V., Geological Society of America special paper.